

# **Geomicrobiology of Pyrite (FeS<sub>2</sub>) Dissolution: Case Study at Iron Mountain, California**

**KATRINA J. EDWARDS**

Department of Geology and Geophysics  
University of Wisconsin-Madison  
Madison, Wisconsin, USA

**BRETT M. GOEBEL**

Department of Plant and Microbial Biology  
University of California, Berkeley  
Berkeley, California, USA

**TERESA M. RODGERS**

**MATTHEW O. SCHRENK**

**THOMAS M. GIHRING**

Department of Geology and Geophysics  
University of Wisconsin-Madison  
Madison, Wisconsin, USA

**MARGARITA M. CARDONA**

**BO HU**

**MOLLY M. McGUIRE**

**ROBERT J. HAMERS**

Department of Chemistry  
University of Wisconsin-Madison  
Madison, Wisconsin, USA

**NORMAN R. PACE**

Department of Plant and Microbial Biology  
University of California, Berkeley  
Berkeley, California, USA

(continued)

Received 28 July 1998; accepted 25 September 1998.

This article is not subject to U.S. copyright laws.

We thank the two anonymous reviewers for their helpful comments, T.W. Arman for providing access to the field site, and Stauffer Management Co. for logistical support. Funding was provided by NSF grant CHE-9521731 and by GSA student research grants to K.J.E.

Address correspondence to Dr. Katrina Edwards, Department of Geology and Geophysics, University of Madison-Wisconsin, Madison, WI 53706, USA.

## JILLIAN F. BANFIELD

Department of Geology and Geophysics  
University of Wisconsin-Madison  
Madison, Wisconsin, USA

*Geomicrobiology of pyrite weathering at Iron Mountain, CA, was investigated by molecular biological, surface chemical, surface structural, and solution chemical methods in both laboratory and field-based studies. Research focused at sites both within and peripheral to the ore-body. The acid-generating areas we have examined thus far at Iron Mountain (solution pH < 1.0, temperature > 35°C) were populated by species other than Thiobacillus ferrooxidans. 16S rDNA bacterial sequence analysis and domain- and species-level oligonucleotide probe-based investigations confirmed the presence of planktonic Leptospirillum ferrooxidans and indicated the existence of other species apparently related to other newly described acidophilic chemolithotrophs. T. ferrooxidans was confined to relatively moderate environments (pH 2–3, 20–30°C) that were peripheral to the ore-body. Dissolution rate measurements indicated that, per cell, attached and planktonic species contributed comparably in acid release. Surface colonization experiments in the laboratory and field indicated that attachment was specific to sulfides instead of to silicates, occurred in crystallographically preferred orientations, and, after cell division, resulted in a monolayer of cells at a maximum density of  $8 \times 10^6$  cells  $\text{cm}^{-2}$ . In situ geochemical characterization throughout the year revealed that the microbial community that controlled acid generation varied and could be correlated with seasonal and spatial fluctuations in geochemical conditions.*

**Keywords** acid mine drainage, dissolution, fluorescence in situ hybridization, low pH, microbial attachment, phylogenetic analysis, pyrite, surface reactions

Biogeochemical dissolution of sulfide minerals exerts a major control on the sulfur cycle, is used in biorecovery of metals, and can be a source of environmental pollution. Interaction between sulfide minerals such as pyrite ( $\text{FeS}_2$ ), water, microorganisms, and air results in acidic, metal-rich waters. When this process is accelerated by mining activities, pollution known as acid mine drainage (AMD) results. However, sulfide dissolution also occurs in the absence of mining (Runnels et al. 1993). A brief history of acid rock drainage and the impact of mining can be found in Nordstrom and Alpers (in press).

Pyrite oxidation in nature is neither a purely chemical nor a purely microbial process. Rather, it is the result of a complex interplay of processes dependent on rock type, mineral structure and chemistry, fluid abundance and chemistry, microbial community, and temperature. Despite the importance of sulfide dissolution over a wide spectrum of Earth environments, the literature is overwhelmingly dominated by studies involving only a few chemolithotrophic species (members of *Thiobacillus* and *Leptospirillum* genera) over a restricted range of environmental conditions (pH 2–3, 20–30°C).

Typically, factors controlling sulfide mineral dissolution have been treated independently and with use of a variety of methodologies. Experimental geochemical measurements of aqueous pyrite oxidation rates are usually normalized to surface area, whereas bioleaching rate measurements using cultured organisms are typically normalized to a slurry density per volume of solution (the surface area not being measured or reported). Reintegration across disciplinary lines is difficult.

Here we present an analysis of the factors controlling natural oxidative pyrite dissolution by combining published results with data from an integrated geochemical and geomicrobiological case study conducted at Iron Mountain, in the West Shasta district, near Redding, CA (Figure 1).

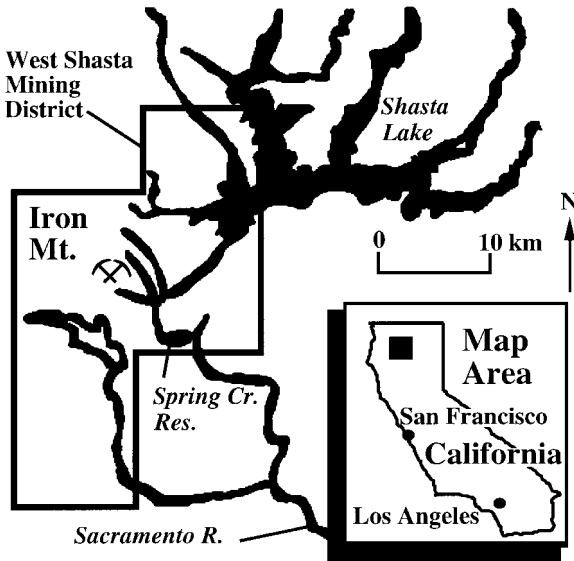


FIGURE 1 Location map of Iron Mountain, California.

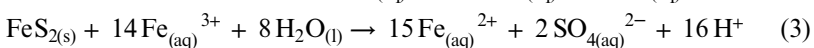
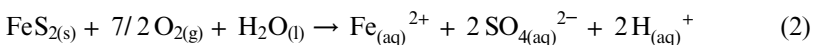
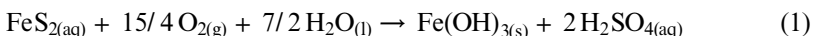
### Aqueous Pyrite Oxidation

Prior laboratory studies have elucidated rate laws and mechanisms of pyrite oxidation by oxygen and ferric iron (Stokes 1901; Garrels and Thompson 1960; Wiersma and Rimstidt 1984; McKibben and Barnes 1986; Moses et al. 1987; Brown and Jurinak 1989; Rimstidt and Newcomb 1992; Williamson and Rimstidt 1994) and have considered the role of  $\text{CO}_2$  as a pyrite oxidation catalyst (Evangelou and Zhang 1995). Reviews can be found in Lowson (1982), Nordstrom (1982), Nordstrom and Southam (1997), and Nordstrom and Alpers (in press).

Although the overall conversion of pyrite to the most-oxidized products is reaction 1 shown in Table 1 and the commonly cited reaction at low pH is reaction 2, in detail sulfur oxidation involves intermediates such as elemental sulfur and sulfoxyanions (thiosulfate, polythionates, and sulfite). However, these intermediates are rarely detected in acidic environments (Nordstrom and Alpers, in press).

Initiation of pyrite oxidation has been proposed to involve ferric ions, which oxidize pyrite 3 to 100 times faster than does oxygen (reaction 3, Table 1; McKibben and Barnes 1986). This reaction is important only at low pH (<4.0), given the low solubility of ferric iron at higher pH values. Under low-pH conditions, the rate-limiting step for reaction 3 is the oxidation of ferrous iron, as shown in reaction 4. However, this reaction is itself rate-limited by pH; that is, the oxidation of ferrous iron slows with decreasing pH (Singer and Stumm 1968).

TABLE 1 Pyrite oxidation reactions



## Microbial Pyrite Oxidation: Direct Versus Indirect Attack

### Laboratory Studies

The mechanisms by which microorganisms accelerate pyrite dissolution under acidic conditions remain contentious. Silverman and Ehrlich (1964) proposed two pathways for metal sulfide oxidation by chemolithotrophic microorganisms, termed direct and indirect attack. Direct attack was used to imply an enzymatic attack by organisms attached to the pyrite surface. However, attached microorganisms are not evidence per se for the existence of the direct mechanism. For example, Sand et al. (1995, 1997; Schippers et al. 1996) have proposed that attached cells produce an exopolysaccharide that complexes with ferric ions specifically, thus generating a local environment rich in pyrite-oxidizing potential. Moreover, specific evidence for an extracellular enzyme system capable of sulfide oxidation has yet to be provided, though such systems have been documented for some iron- (and manganese) oxidizing bacteria (Corstjens et al. 1992; Tebo et al. 1997). The indirect attack of pyrite is assumed to proceed via chemical oxidation of pyrite by  $\text{Fe}^{3+}$ . In this instance, attached or planktonic microorganisms generate ferric ions via the energetic oxidation of ferrous ions. Although there is evidence for oxidation by both attached and planktonic species, specific information regarding the kinetics and chemistry of sulfide dissolution remains obscure.

Regardless of the enzymatic or nonenzymatic nature of the reaction, microbial attachment to sulfide surfaces impacts oxidative dissolution. Dissolution in the presence of attaching organisms results in local, crystallographically controlled etching (Bennet and Tributsch 1978; Konishi et al. 1990; Edwards et al. 1998), which does not occur in the presence of exclusively planktonic chemolithotrophs (Edwards et al. 1998). Microorganisms attach to sites of high surface energy, such as scratches (Figure 2), pits, grooves, and steps. Site specificity for attachment at the reactive regions of the sulfide surface, in combination with the creation of localized microenvironments between cells and the surface, probably accounts for the morphological expression of dissolution observed in the presence of attaching organisms.

In cases where attachment occurs away from surface scratches, cell orientation on the surface occurs in nonrandom directions. Fourier transforms of images of organisms attached to pyrite surfaces indicate two distinct trends at  $90^\circ$ . An example of this is shown in Figure 3, where alignment is parallel to the  $\langle 100 \rangle$  crystallographic directions. Alignment also occurs parallel to  $\langle 110 \rangle$ . Dissolution pits associated with attached cells are euhedral, with pit edges parallel to  $\langle 100 \rangle$  and  $\langle 110 \rangle$  (Figure 4). Attachment is specific for pyrite compared with silicate inclusions. Surface attachment details relative to the crystallographic directions of a pyrite cube are summarized in Figure 5. These data strongly suggest a crystallographic control on surface attachment and dissolution by microorganisms.

Although attachment is frequently seen approximately equally parallel to the [001] and [010] directions contained within a (100) pyrite surface, steps do not occur in equal abundance parallel to these directions (because of pyrite symmetry). Consequently, step distribution alone does not explain the observed cell orientations and distributions. The {100} face of a pyrite cube consists of sites occupied by Fe or S dimers in an alternating checkerboard-like pattern (Figure 6). Eggleston et al. (1996) found that oxidation proceeds across the {100} pyrite surface along fronts parallel to the {100} and {110} atomic planes (see below for further discussion). Thus, cell orientation may occur in response to the resulting oriented zones of enhanced reactivity.

### Field Colonization

Field colonization experiments were conducted at the Iron Mountain field site, with use of pyrite "growth substrates," to study surface evolution and attachment specificity (Edwards

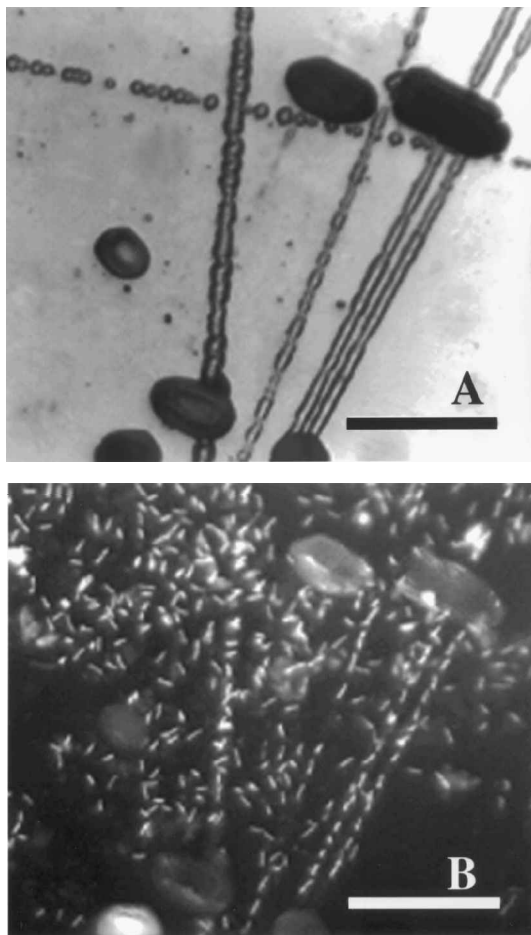


**FIGURE 2** (A) Reflected light image of pyrite surface after incubation in enrichment culture from Iron Mountain (see text). The scratches formed during polishing of the crystal face. Scale bar is 25  $\mu\text{m}$ . (B) Fluorescent image of cells clustered along a scratch on a polished pyrite crystal, after 1 week of incubation in enrichment culture from Iron Mountain. Cells are stained with 4',6-diamidino-2-phenylindole (DAPI; Kapuscinski 1995) for observation by ultraviolet (UV) epifluorescent microscopy with a Leica LEITZ DMRX microscope. Scale bar is 25  $\mu\text{m}$ .

et al. 1998). Microbial attachment, surface etching, and preferential orientation were found to be similar to those observed in the laboratory. Attachment is clearly common, even at very low pH ( $< 1.0$ ), and results in surface roughening at a different scale than seen in the presence of planktonic species. The detailed nature of the competitive advantage conferred by surface attachment (justifying the expenditure of energy needed to form attachment polymers) remains an important, unresolved question.

## Surface Studies: Pyrite Oxidation at the Atomic Level

### *Previous Work*

Although aqueous chemistry studies have quantified overall reaction rates of pyrite oxidation, the rate-limiting steps occur at pyrite surfaces. Different surface sites can differ in

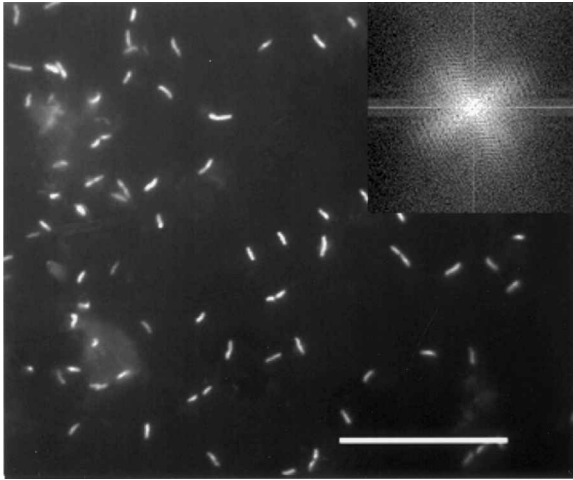


**FIGURE 3** Organisms adhering to cubic pyrite surface, stained with DAPI (see Figure 2) and imaged in reflected UV fluorescence. Upper right: example Fourier transform image of organisms adhering to this surface, showing two distinct trends in alignment at  $90^\circ$  to each other and parallel to  $\langle 100 \rangle$ . Scale bar is  $25 \mu\text{m}$ .

reactivities because of differences in structure, composition, number of defects, or crystallographic face. In bulk-solution experiments these effects have been recognized and quantified to some degree (e.g., Martello et al. 1994). However, surface-scanning techniques provide important details on the structure and composition of surfaces necessary to understand how reactions proceed at the atomic level. X-ray photoelectron spectroscopy (XPS) and Raman spectroscopy provide bulk surface-speciation information, whereas atomic force microscopy (AFM) and scanning tunneling microscopy (STM) provide atomic-level resolution of surface features.

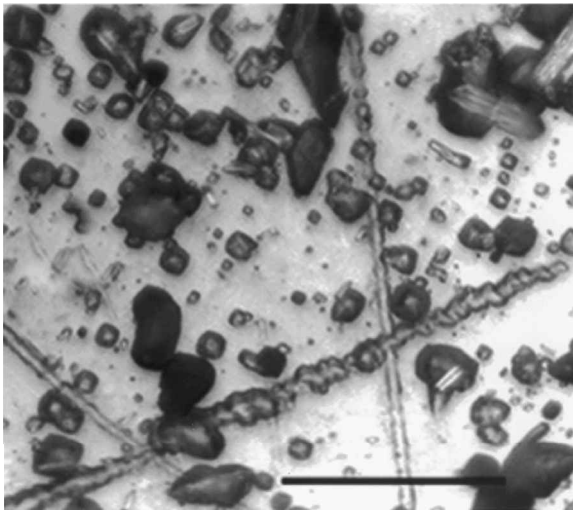


**FIGURE 4** Reflected light image of euhedral dissolution pits that develop on pyrite surfaces after incubation in enrichment culture from Iron Mountain (see text for discussion). Scale bar is  $25 \mu\text{m}$ .

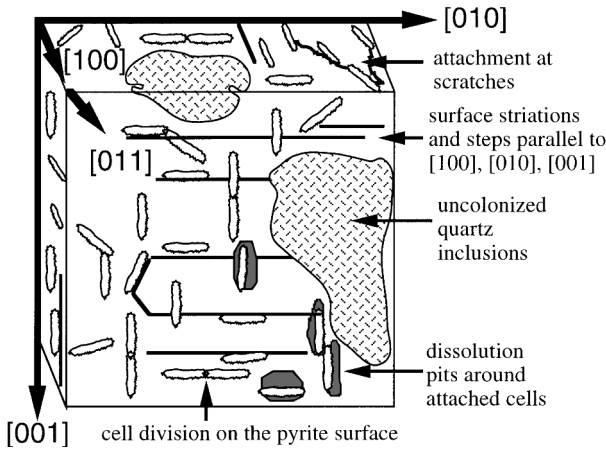


**FIGURE 5** Details of surface attachment relative to the crystallographic directions of a pyrite cube. The [100], [010], and [001] directions are parallel to the cube edges; the [110], [101], and [011] directions are diagonal to cube edges.

XPS and Raman spectroscopy have confirmed that under acidic conditions, iron is leached from pyrite, leaving a sulfide-rich layer (disulfide, monosulfide, and polysulfides; Sasaki 1994; Nesbitt and Musir 1994, Sasaki et al. 1995). Production of unstable sulfoxyanions, having oxidation states intermediate between sulfur and sulfate, have been detected unambiguously only by surface-spectroscopic techniques. The abundance of the sulfoxyanions depends on the solution pH, with polythionates dominating at low pH, thiosulfate at intermediate pH, and sulfite at the highest pH values (Goldhaber 1983; Moses et al. 1987). In the presence of ferric iron, sulfoxyanions are not detectable (Moses et al. 1987).

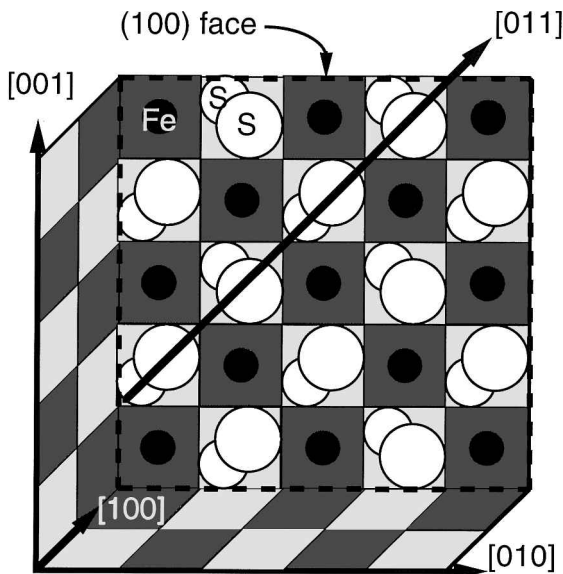


**FIGURE 6** Schematic representation of a {100} pyrite surface (dashed outline). The center of mass of the sulfide moiety is in the same plane as the Fe atoms, although individual S atoms are not.

As noted above, Eggleston et al. (1996) used STM to observe surface oxidation patterns; they found that oxidation proceeds in patches and typically follows the  $\langle 100 \rangle$  and  $\langle 110 \rangle$  crystallographic directions. The percentage of oxidized surface sites was quantified with XPS. Surface oxidation models based on these analyses suggest that the reaction proceeds autocatalytically, with the probability of oxidation at any particular site being proportional to the number of nearest oxidized neighbors. Studies such as these elucidate microscopic mechanisms for oxidation patterns observed in laboratory and natural samples.

### XPS and Raman Studies

A comparison of rates and mechanisms on samples reacted under biotic and abiotic conditions should provide information crucial to understanding microbially induced oxidation. For surface chemistry experiments we used natural, uncut, single pyrite crystal faces (Ward's Scientific). "Biotic" experiments used enrichment cultures from Iron Mountain. "Abiotic" experiments were done in uninoculated media of the same composition as biotic experiments. Abiotic and biotic experiments were done at pH and temperature conditions relevant to the field site (pH  $\sim 0.7$ ,  $42^\circ\text{C}$ ), with at least one natural face exposed for analysis. Pyrite was prepared by immersion in 0.52 M HCl for 8–10 h to remove surface oxides and impurities, then sonicated in 70% (by vol) ethanol for  $\sim 20$  min. XPS analysis directly after this procedure confirmed the efficiency of the procedure for surface cleaning (data not shown). After treatment with HCl, samples were rinsed with distilled water and stored in 70% ethanol before use ( $< 1$  week). XPS analysis after 1 week confirmed that no detectable chemical changes took place on the samples' surfaces during storage in ethanol after the acid treatment (data not shown).

The XPS system used for these experiments was from Physical Electronics with a monochromatized Al K $\alpha$  source and a multichannel detector array. Raman spectroscopy was performed by focusing light from a 200 mW argon-ion laser (at 514 nm) onto a natural face on the sample; scattered light was collected by using an  $f/1.8$  imaging spectrograph (Kaiser Optical) and a cooled charge-coupled device array detector (Photometrics). The STM, feedback control electronics, and bipotentiostat were designed and built by Higgins and Hamers (1995).

A visual comparison showed that pyrite crystals reacted in the presence of microorganisms in solution (biotically) were visibly tarnished, whereas those reacted abiotically remained free of surface deposits. The Raman spectra (Figure 7) show the surface

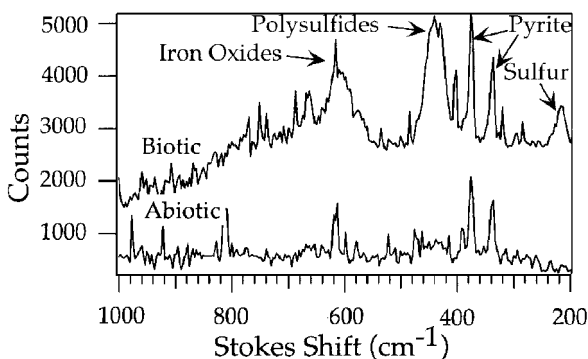


**FIGURE 7** Raman spectra of biotically and abiotically reacted samples. Raman shifts are in relative wave numbers; intensities are in arbitrary units. The higher background in the biotically reacted sample is due to the greater surface roughness, resulting from incubation in the presence of organisms that attach to pyrite (see Figure 4).

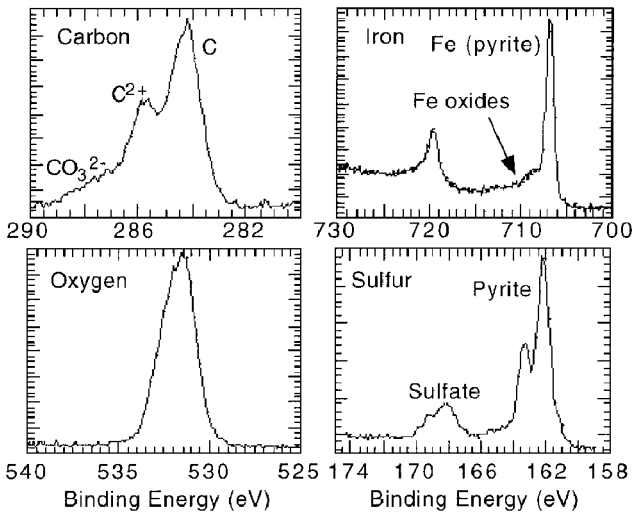


**FIGURE 8** XPS analyses of surface compositions of biotically reacted samples.

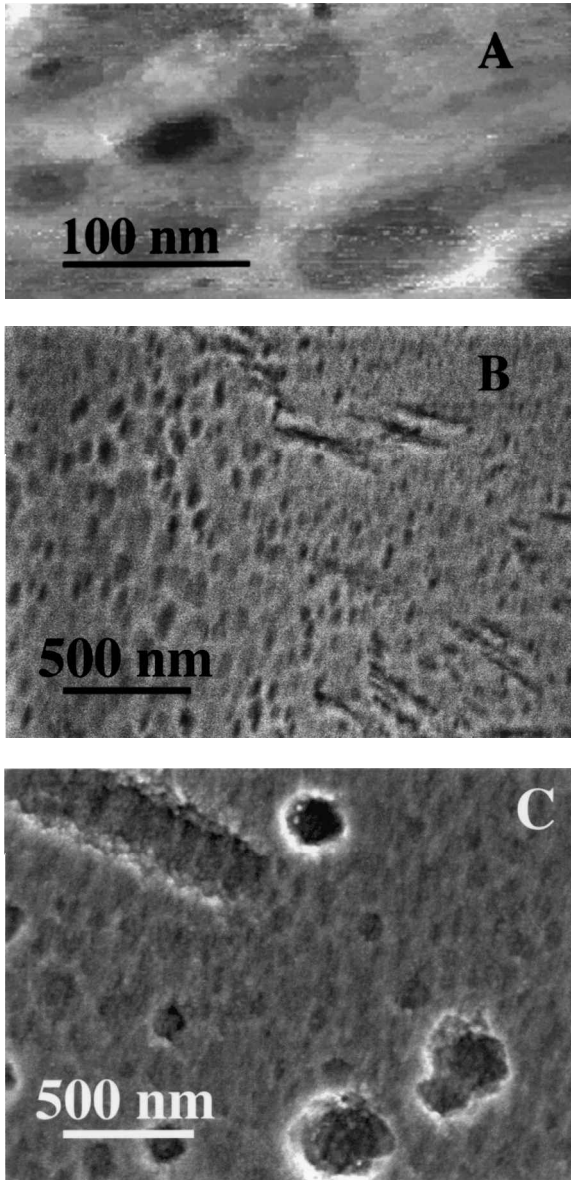
compositions of both samples after reaction. Stokes lines at  $336$  and  $375\text{ cm}^{-1}$  are observed in both samples and arise from bulk pyrite (Mernagh and Trudu 1993). On the biotically reacted samples, additional peaks at  $214$ ,  $430$ , and  $440\text{ cm}^{-1}$  are observed from surface reaction products. The broad band at  $420\text{--}450\text{ cm}^{-1}$  is attributed to multiple polysulfide species (Mycroft et al. 1990), whereas the peak at  $214\text{ cm}^{-1}$  is attributed to elemental sulfur on the surface. The peaks in the  $615\text{ cm}^{-1}$  region are from iron oxides (Thibeau et al. 1978). All these products are virtually absent in the abiotically reacted sample.

Figure 8 shows the corresponding XPS surface analysis of the biotically reacted sample. In XPS spectra, the lines corresponding to a particular element undergo small shifts in energy because of changes in the local oxidized state. Carbon is clearly present in at least three chemical forms. The peak at  $284\text{ eV}$  arises from carbon in a neutral (alkane-like) state; the one at  $286\text{ eV}$  arises from an oxidation product; and the shoulder near  $288\text{ eV}$  arises from carbon in a carbonate-like form. The XPS spectra from the biotically reacted sample show iron in a high oxidation state (appropriate for iron oxide) and oxidized forms of sulfur, particularly sulfate. These data demonstrate that a consequence of reaction in the presence of microorganisms is the rapid development of oxidized Fe and S compounds on pyrite surfaces.

### ***STM and Scanning Electron Microscopy (SEM) Studies***

Isotope studies suggest that ferric ion directly oxidizes the pyrite surface (Taylor et al. 1984a,b). Planktonic organisms that participate in the oxidation of pyrite “indirectly” do so by controlling the ferric ion concentration in solution. To study the impact of the ferric ion concentration on surface morphology and dissolution rates, we conducted comparison studies on surfaces exposed or not exposed to ferric ion.

Figures 9 and 10 present surface topography for samples treated with ferric ion initially present or treated without ferric ion. Figure 9A is a STM image of acid-treated pyrite; Figure 9B is a SEM image of a similarly treated surface. Both images reveal pits  $50\text{--}100\text{ nm}$  in diameter across the surface. A surface treated similarly for longer periods, shown in Figure 9C, reveals larger pits at the surface. This lateral pit growth suggests preferential dissolution from the edges of the pits. Because dissolution is likely to be sensitive to surface



**FIGURE 9** (A) STM image of pyrite (100) surface reacted with 0.52 M HCl for 1 day. Pit edges are parallel to  $\{100\}$ . (B) SEM image of pyrite (100) surface reacted with pH 1.5  $\text{H}_2\text{SO}_4$  for 1 day. (C) SEM image of pyrite (100) surface reacted with pH 1.5  $\text{H}_2\text{SO}_4$  for 1 week.

imperfections such as steps and dislocations (Higgins and Hamers 1995, 1996), pitting is expected to strongly affect the dissolution rate by producing sites of high reactivity and increasing surface area. Figures 10A and 10B are SEM images at different magnifications of a surface reacted with 0.10 M ferric sulfate solution for the same length of time as in Figure 9C. Although there is no visible surface pitting, substantial formation of surface deposits is observed. These types of deposits may be analogous to surface oxidation products produced in biotically reacted samples.

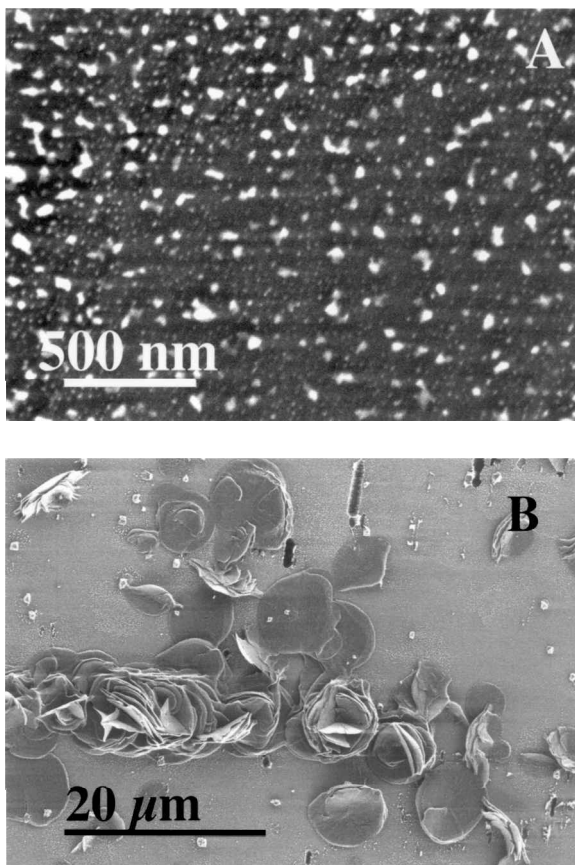


**FIGURE 10** (A) SEM image of pyrite (100) surface reacted with 0.10 M  $\text{Fe}_2(\text{SO}_4)_3$  at pH 1.5 for 1 week. (B) SEM image of the same sample under greater magnification.

### Quantitative Dissolution by Microorganisms

The oxidation of exposed sulfide minerals is greatly influenced by the activities of those microorganisms that can use reduced iron or sulfur (or both) for energy. The cycling of  $\text{Fe}^{2+} \rightarrow \text{Fe}^{3+}$  by microorganisms is thought to be the mechanism by which reaction 4 (Table 1) is catalyzed in low-pH environments. Estimates of the biotic dissolution rate range from  $\sim 8.8 \times 10^{-8} \text{ mol m}^{-2} \text{ s}^{-1}$  (at 25°C; Olson 1991) to  $\sim 1.5 \times 10^{-5} \text{ mol m}^{-2} \text{ s}^{-1}$  (at 42°C; Edwards et al. 1998).

Most experiments on microbial pyrite oxidation rates have been done at 25°C and pH values of  $\sim 2$ , where growth of *T. ferrooxidans* is optimized. However, the rates measured at these temperatures are not always reflective of environmental oxidation rates. Additionally, in these environments, *T. ferrooxidans* and other Thiobacilli are clearly not always the predominant chemolithotrophs. Under the more extreme pH and temperature conditions expected at certain sites of significant acid generation, other taxa may, and indeed do, dominate (Rawlings and Kusano 1994; Goebel and Stackebrandt 1994a,b; Schrenk et al. 1998; see also below). Members of the bacterial genera *Sulfobacillus*, *Leptospirillum*, *Acidimicrobium*, and *Thiomonas*; numerous unnamed isolates; and members of the archaeal genera *Sulfolobus*, *Acidianus*, *Metallosphaera*, and *Sulfurococcus* may all contribute significantly to sulfide dissolution (see below for further discussion). The possibility

that as-yet-unstudied species are also present and metabolically active in acidic environments may result in measured laboratory oxidation rates that diverge considerably from environmental rates.

In a recent review, Nordstrom and Alpers (in press) analyzed the biotic and abiotic data available and concluded that pyrite oxidation rates in nature are limited by the rate at which iron is oxidized and thus by the abundance of chemolithotrophic species. They argue that natural rates reflect the indirect rate, which involves acceleration of dissolution by organisms that oxidize ferrous iron in solution. This analysis involved inferred cell populations and relied on information drawn from multiple studies. No special significance was attributed to attached cells, although in many environments cells clearly are frequently attached, and surfaces evolve differently in the presence of attached cells (see above). Rates normalized to cell numbers and surface area have not been reported, however, and a direct comparison between these rates for attached and planktonic cells is thus not possible.

To quantify oxidation rates per cell at conditions relevant to Iron Mountain, we conducted experiments with mixed enrichment cultures from the Richmond mine (Edwards et al. 1998). The experiments were done at average field conditions (42°C, pH 0.7) and using single pyrite cubes of uniform size to constrain available surface area. Two separate enrichment cultures were used, one containing bacteria that attached to pyrite surfaces and one that did not. Both cultures contained *L. ferrooxidans* as a planktonic phase and were devoid of *T. ferrooxidans* (determined by using species-specific oligonucleotide probes; see below).

Total rates of solubilization and growth were significantly higher in enrichments containing organisms that attach to pyrite surfaces than in the one without ( $1.5 \times 10^{-5}$  mol  $m^{-2} s^{-1}$  compared with  $2.0 \times 10^{-6}$  mol  $m^{-2} s^{-1}$ , respectively). However, the total iron released per organism per day was approximately equal in the two cultures,  $\sim 10^{-7}$   $\mu$ mol of Fe cell $^{-1}$  day $^{-1}$ . Thus these experiments do not suggest any clear metabolic advantage gained by attachment, at least over the duration of these experiments. However, as discussed above, attachment results in quite different surface morphology evolution. The distinct pitting that occurs in the presence of organisms that attach to pyrite, pitting that is absent in their absence, ultimately results in an overall increase in surface area. Available surface area is one of the most important controlling factors in pyrite dissolution (see above). Thus attachment as a mechanism by which microorganisms increase substrate availability may be an important control in the formation of AMD.

## Biodiversity of Microbial Pyrite Oxidation

Although most laboratory studies to date have concentrated on the role of *T. ferrooxidans* in sulfide dissolution, diverse communities of acidophilic organisms may influence leaching rates. Depending on the prevailing conditions, different suites of microorganisms will be selected for. For example, as is well documented, under certain conditions (particularly at pH < 1.8, or a high Fe $^{3+}$ :Fe $^{2+}$  ratio, or both), leptospirilla are likely to predominate over *T. ferrooxidans* in the temperature range of 20–45°C (Goebel and Stackebrandt 1994a, 1995; Helle and Onken 1988; Norris 1983, 1988; Rawlings 1995; Sand et al. 1992; Schrenk et al. 1998). It is therefore essential to investigate the diversity of microorganisms associated with pyrite dissolution by using molecular techniques that circumvent many of the biases associated with traditional enrichment and isolation techniques (Amann et al. 1995; Pace et al. 1986). To date, the limited applications of molecular methods to acidic metal-leaching environments suggest these communities consist of taxa that are readily obtained by culturing techniques (Goebel and Stackebrandt 1994b, 1995; Pizarro et al. 1996; Rawlings 1995; Vásquez and Espejo 1997). In this respect, acidic environments are unique; all other

environments studied with use of similar approaches have yielded a wealth of novel 16S rRNA sequences, often only distantly related to those of cultured organisms (P. Hugenholtz et al. 1998). However, given that only a limited number of samples have been examined so far, it is premature to conclude that all microorganisms in acidic metal-leaching environments are readily cultivated.

Samples collected from two sites at Iron Mountain were analyzed by Rodgers et al. (1996)—one (TRA) from a runoff stream located peripheral to the Iron Mountain ore-body (20°C, pH 2.4, 4.3 mS cm<sup>-1</sup>), and another (TRB) from a stream located within the Richmond mine 5-way (49°C, pH 0.5, 106 mS cm<sup>-1</sup>). Total DNA was extracted and purified essentially according to the direct-lysis protocol of Barns et al. (1994). Additional details of clone library generation, clone screening, and sequencing are discussed by Rodgers (1996; and ms. in preparation) and are available from the authors on request.

### Phylogeny

In this paper we report a reanalysis of the sequences obtained by Rodgers et al. (1996; and ms. in preparation), using the suite of programs associated with the ARB software package (O. Strunk et al., ms. submitted) and the Ribosomal Database Project (RDP; Maidak et al. 1997). Initially, clones were screened for chimeric artifacts by using the CHECK\_CHIMERA program of the RDP and by manual examination for secondary structure anomalies. Gapped-BLAST analysis was used to search the GenBank database for putative phylogenetic relatives for each clone (Altschul et al. 1997). The results of the gapped-BLAST search were used to select 16S rRNA sequences with which to manually align the clones sequences; both primary and secondary structural information were considered. Aligned sequences were inserted into a phylogenetic tree containing >8000 SSU rRNA sequences by using the Parsimony Insertion tool of the ARB program (Strunk and Ludwig, submitted). This approach allows a rough phylogenetic comparison of sequences that do not necessarily contain overlapping regions of sequence. This situation is common when dealing with sequences generated from environmental clones, because full-length SSU rRNA sequences often are not determined. More extensive analyses using neighbor-joining, maximum parsimony, and maximum likelihood algorithms were performed on certain groups as indicated.

Rodgers et al. (1996) obtained a total of 63 16S rRNA clones from the two clone libraries, TRA and TRB (see above). To simplify analyses, clones that had >98% sequence identity were treated as a group, and a type-sequence was chosen to represent that group (Table 2).

Initially, gapped-BLAST analysis (Altschul et al. 1997) was used to estimate the relationship of the clones to other known bacterial 16S rRNA sequences. With one exception (a mitochondrial-like sequence, TRB2), all clones shared >90% similarity with some other bacterial 16S rRNA sequence in the GenBank database (Table 2); 16S rRNA gene sequences obtained from environmental samples often exhibit <90% or even only 80% identity to known sequences. In fact, many of the sequences obtained in this study were >97% identical with 16S rRNA sequences from organisms previously isolated from acidic environments. This result supports the previous observation that these communities consist predominantly of taxa that are readily obtained in culture (Goebel and Stackebrandt 1994b, 1995; Pizarro et al. 1996; Rawlings 1995; Vásquez and Espejo 1997). However, no 16S rRNA sequences related to those from *T. ferrooxidans* or *T. thiooxidans* were recovered from either of the samples examined. Additionally, a large proportion (~40%) of clone sequences were highly similar (>97% sequence identity) to those of organisms not previously found in acidic biotopes. This suggests that our knowledge of diversity in these ecosystems

**TABLE 2** Distribution and affiliation of TR-series clones to known bacterial taxa

Type sequence	Clones sharing > 98% identity to type sequence		Bacterial division or affiliation <sup>c</sup>	Closest match (gapped-BLAST) <sup>d</sup>		Accession number
	TRA clones <sup>a</sup>	TRB clones <sup>b</sup>		Organism	%	
TRA1-6	2-9, 3-1, 3-4, 3-16, 4-4		$\gamma$ -Proteobacteria	<i>Serratia fitcaria</i>	99	AF047634
TRA1-10	1-11, 3-2, 3-3, 5-7, 5-8, 4-13	15, 16, 17, 39, 60	Nitospira	<i>Leptospirillum ferrooxidans</i>	L15	AF047641
TRA1-16			BCF	<i>Oribaculum catoniae</i>	95	AF047636
TRA1-20			Chloroplast	<i>Ochromonas danica</i> chrysoplast	91	AF047635
TRA2-7			$\gamma$ -Proteobacteria	<i>Stenotrophomonas maltophilia</i>	97	AF047649
TRA2-10			Actinobacteria	<i>Acidimicrobium ferrooxidans</i>	93	AF047642
TRA3-15			$\beta$ -Proteobacteria	<i>Comamonas testosteroni</i>	100	AF047638
TRB3-20	4-2, 4-3, 4-17, 5-20	9, 34, 35, 55, 79, 80, 81, 83	$\beta$ -Proteobacteria	<i>Kingella kingae</i>	91	AF047644
TRA5-3	4-14		$\gamma$ -Proteobacteria	<i>Psychrobacter glacincola</i>	92	AF047645
TRB2			$\alpha$ -Proteobacteria	Mitochondrion 16S rRNA	n.d. <sup>e</sup>	AF047650
TRB3	2-3, 5-5	23, 37, 54	$\alpha$ -Proteobacteria	<i>Acidiphilium</i> strain C	97	AF047648
TRB18		22, 49, 52	Chloroplast	<i>N. plumaginifolia</i> chloroplast	99	AF047637
TRB25	1-17, 3-5	19, 24, 48, 71	$\alpha$ -Proteobacteria	<i>Acidiphilium angustum</i>	99	AF047643
TRB32			$\beta$ -Proteobacteria	<i>Leptothrix discophora</i> SS-1	98	AF047647
TRB41			$\alpha$ -Proteobacteria	<i>Ochrobacterium anthropi</i>	99	AF047640
TRB50		65	Actinobacteria	<i>Aureobacterium liquefaciens</i>	99	AF047639
TRB82			Acidobacteria	<i>Acidobacterium capsulatum</i>	97	AF047646
Chimeras		4, 4-1				

<sup>a</sup>Clone series TRA originates from pH 2.5 stream sample.

<sup>b</sup>Clone series TRB originates from pH 0.5 pyritic sediment sample.

<sup>c</sup>As determined by detailed phylogenetic analysis (see text).

<sup>d</sup>Altschul et al. (1997).

<sup>e</sup>Not detected by BLAST analysis.

may be limited by previous culturing approaches (for details, see Table 2). This possibility is discussed below. The phylogenetic positions of selected clones are presented in Figures 11 and 12. Almost 50% of the total number of clones were closely related (>97% sequence identity) to members of the genera *Leptospirillum* and *Acidiphilium* (Figures 11A and 11B). All of the leptospirilla clones, represented by clone TRA1-10, are >99% identical to one another, with this phylotype being found in both of the samples examined. Moreover, these clones were almost identical in sequence to the 16S rRNA sequence obtained from *L. ferrooxidans* strain L15, the first strain of *Leptospirillum* isolated (Markosyan 1972). Goebel and Stackebrandt (1995) have suggested that *L. ferrooxidans* strain L15 may represent an "atypical" strain of *Leptospirillum*, because all other isolates sequenced to that time formed a tight cluster (Group II, Figure 11B) separate from *L. ferrooxidans* strain L15 (Group I, Figure 11B). The current data make evident, however, that under certain environmental conditions populations of leptospirilla of the Group I type predominate over those of the Group II type. The forces driving this selection process remain to be investigated.

Two groups of clones related to members of the genus *Acidiphilium* were recovered from both of the samples examined (Table 2 and Figure 11A). Members of this genus (and the genus *Acidoceella*) are common heterotrophic inhabitants of acidic metal-leaching habitats (see Johnson and Roberto [1997] for a recent review). Sequences represented by the clone TRB25 were almost identical to 16S rRNA sequences of *Acidiphilium rubrum*, *Acidiphilium angustum*, and *T. acidophilus*, whereas sequences represented by clone TRB3 had no specific affiliation with any *Acidiphilium* species previously sequenced (Figure 11A). The two clone groups are ~97% identical in sequence. However, one cannot predict whether these sequences originated from closely related species, the same species, or even the same organism, because sequence heterogeneity among *rrn* operons is well documented (Stackebrandt and Goebel 1994; Wang et al. 1997) and is common in environmental 16S rRNA clone studies that use the polymerase chain reaction (PCR; Giovannoni et al. 1990).

Two of the clone-types (clone TRA2-10 and TRB82) are closely related to acidophiles that have obscure roles in acidic environments. Clone TRA2-10 forms a monophyletic clade with *Acidimicrobium ferrooxidans* (Clark and Norris 1996) and *Ferromicrobium acidophilus* (Johnson and Roberto 1997) at the base of the high-G+ C gram-positive phylum (recently named the *Acidobacteria* by Stackebrandt et al. 1997) (Figure 12A). Although not specifically related to either of these two recently described acidophiles, there is strong bootstrap support for the monophyly of this group. By physiological inference, the clone TRA2-10 may originate from an as-yet-uncultivated group of acidophilic, mixotrophic, iron-oxidizing bacteria.

Clone TRB82 forms a close affiliation with the acidophilic heterotroph *Acidobacterium capsulatum* (Kishimoto et al. 1991; Hiraishi et al. 1995) and a group of environmental 16S rRNA clone sequences (TM-series) recovered from a pH 2.7 peat bog sample (Rheims et al. 1996) (Figure 12B). Clone MC13, recovered from a pH 4 forested soil (Stackebrandt et al. 1993), is also shown in Figure 12B. Although the bootstrap-supported monophyly of this group in Figure 12B would suggest acidophily as a unifying trait within this cluster, a large number of environmental clone sequences originating from various nonacidic sources have recently been described (Borneman et al. 1996, Borneman and Triplett 1997; Kuske et al. 1997; Ludwig et al. 1997; Wise et al. 1997), and the phylogeny of this large new phylum/division (represented by only three cultivated species) is in a state of flux (Hugenholtz et al. 1998).

Many of the 16S rRNA gene sequences recovered in the study of Rodgers et al. (1996) were closely related (95–100% sequence identity) to microorganisms not previously isolated from acidic environments (Table 2). Examples of these (based on type sequence) include clone TRA1-6, 99% identical to the 16S rRNA of members of the *Escherichia/Shigella*

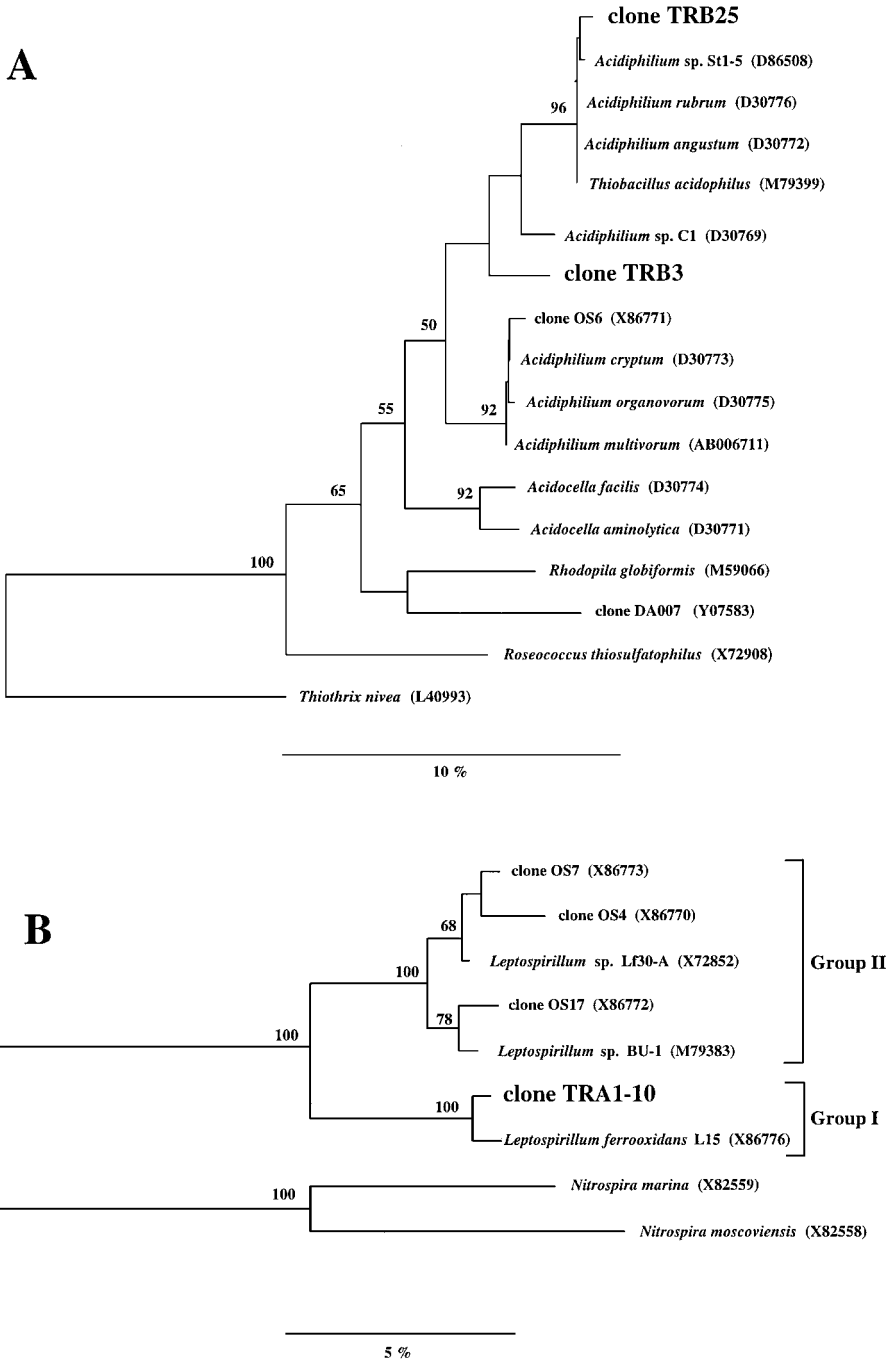


**FIGURE 11** Evolutionary distance dendrograms of the *Acidiphilium/Acidocella* (A) and *Leptospirillum* (B) clades, showing the relative position of representative TR-series clones (shown in larger type) within these groups. The numbers at branches indicate bifurcations that had >50% bootstrap support by the neighbor-joining algorithm. Scale bars represent 10% (A) or 5% (B) sequence divergence.

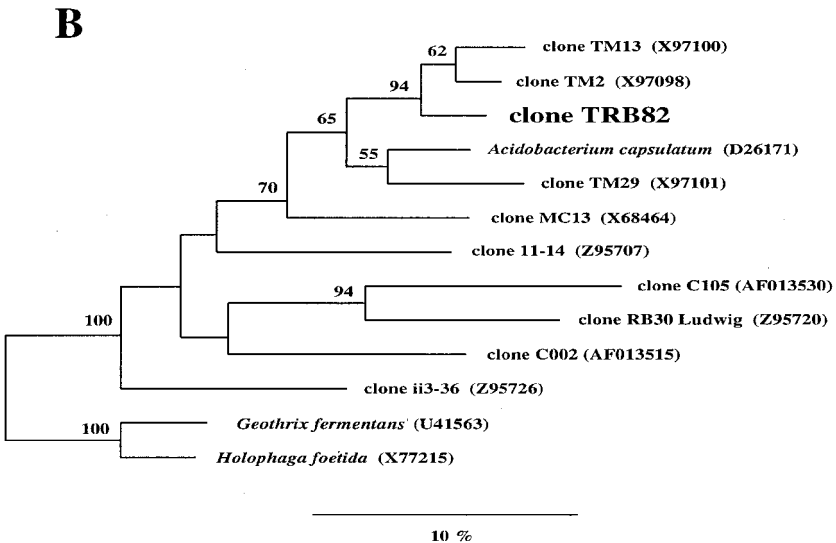
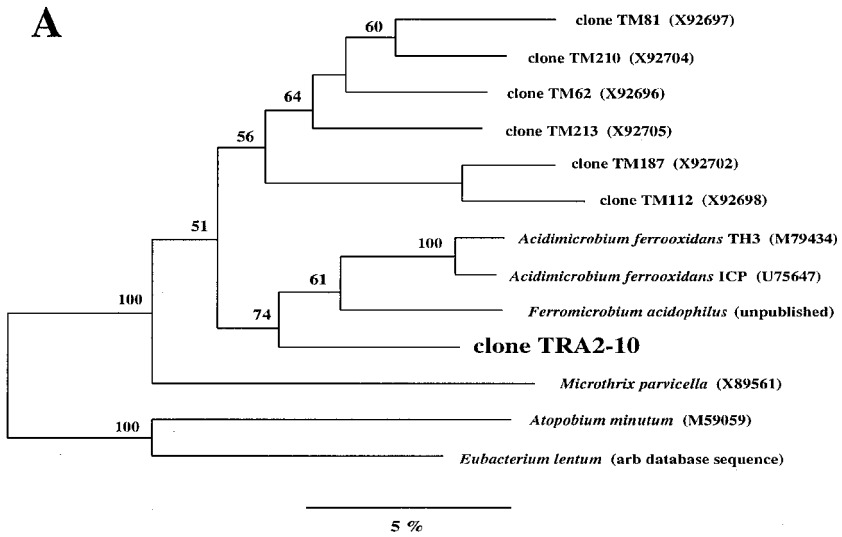


**FIGURE 12** Evolutionary distance dendrograms of the *Acidimicrobium* (A) and *Acidobacterium* (B) clades showing the relative position of representative TR-series clones within these groups. The numbers at branches indicate bifurcations that had > 50% bootstrap support by the neighbor-joining algorithm. Scale bars represent 5% (A) or 10% (B) sequence divergence.

clade of the *Enterobacteriaceae*; clone TRA3-15, with 100% identity to the 16S rRNA of *Comomonas testosteroni*, a commonly isolated soil heterotroph; clone TRB41, with 99% sequence identity to the 16S rRNA of *Ochrobacterium anthropi*, a common clinical isolate and close relative of members of the genus *Brucella*; and clone TRB50, with 99% sequence identity to the 16S rRNA of *Aureobacterium liquifaciens*, an organism previously isolated from dairy products and equipment but also found in soil. Moreover, the group of sequences represented by clone TRB18 are very close relatives (99% sequence identity)

to tobacco plant chloroplasts. It is, therefore, difficult to conclude confidently that the organisms from which the sequences were recovered are indigenous and metabolically active in these acidic systems (and thus potentially involved with the pyrite oxidation process), instead of being introduced as the result of contamination. Although this study was performed by using stringently aseptic technique, the use of PCR to recover sequences from the environment is fraught with potential contamination issues (see Wilson [1997] for a recent review). Several sources of contamination are possible, particularly in low-biomass environments. DNA (or cells) may enter from nonacidic environments via aerial or flow-in sources, although “naked” DNA would most likely undergo rapid acid hydrolysis under the extreme acidity of this environment. Despite the inclusion of negative controls for all PCR reactions (results all negative), a negative template control was not performed during DNA extraction and purification. Therefore, we cannot judge whether or not contamination may have occurred during sample preparation (from surroundings or reagents). Some evidence indicates that contamination during DNA preparation from environmental samples occurs even when aseptic technique is used (Tanner et al. 1998). Future studies will aim to determine whether contamination is a significant issue for clonal analyses of acidic environments and, if possible or necessary, how to minimize these problems.

The ability to oxidize iron, sulfur, and organic material under acidic (< pH 3) conditions is a polyphyletic characteristic (Lane et al. 1992), making it possible that the 16S rRNA clone sequences obtained in this study originated from metabolically active acidophiles. Examples of this are the clones represented by TRA2-7 and TRA5-3 (Table 2). Although neither of these clone groups is >97% identical to cultured species, they cluster in the vicinity of two recently isolated organisms, strains ES1 and ES2 (Emerson and Moyer 1997) and BrG3 (Straub et al. 1996)—both of which are capable of iron oxidation, although not under highly acidic conditions or, in the case of strain BrG3, under anaerobic conditions only (tree not shown). This suggests a possible involvement of iron in the metabolism of the organisms from which these 16S rRNA sequences originated.

Despite substantial differences in the temperature, pH, and conductivity (hence metal-loading) between the two samples examined, there was considerable overlap in the clone-types obtained from each sample. In particular, the same clone-groups related to the genera *Acidiphilium* and *Leptospirillum* were recovered from both samples (Table 2). This suggests that these commonly isolated acidophiles may persist under the broad physicochemical extremes present at the Iron Mountain site. However, since the metabolic activity of organisms in situ cannot be judged on the basis of clone-library data, any inferences of activity must be substantiated by other means.

### ***Fluorescent In Situ Hybridization (FISH)***

Given the inherent biases associated with environmental clone-library generation using PCR, the frequency of the sequences in the clone libraries examined in this study (Table 2) is unlikely to represent the abundance percentage of the corresponding organisms in situ. Potential biases can arise from several sources, including small sample size, differences in *rrn* copy number between taxa, selective lysis and recovery of genomic DNA, contamination (see above), and differential amplification by PCR (Suzuki and Giovannoni 1996; Farrelly et al. 1995; Reysenbach et al. 1992). We have, therefore, been using the 16S rRNA gene-cloning step as a means of collecting environment-specific 16S rRNA sequence data from which taxon-specific hybridization probes can be designed. In this way, temporal and spatial distributions of specific taxa can be determined directly (e.g., Schrenk et al. 1998). Moreover, 16S rRNA sequences obtained by cloning allow us to pose hypotheses concerning the ecology of acidic environments and direct in situ experimentation.

Samples for analysis by FISH were collected in January, March, July, September, and November 1997. Sample collection sites fit into two categories according to environmental conditions, similar to those described above. In general, sites located within the Richmond mine (in contact with the ore-body) had pH values of 0–1, temperatures of 40–50°C, and conductivities of 80–120 mS cm<sup>-1</sup>. Sites outside of the mine (peripheral to ore-body) had pH values of 2–4, temperatures of 10–30°C, and conductivities of 1–10 mS cm<sup>-1</sup>. Samples of water, slime, and sediment were collected from each locality, when possible. Samples were hybridized with probes specific for the species *L. ferrooxidans* and *T. ferrooxidans* and at the domain level for Bacteria, Eukarya, and Archaea. *L. ferrooxidans* probes used in this study were based on SSU rRNA gene sequences for 12 *L. ferrooxidans* clones from Iron Mountain obtained by the above-mentioned phylogenetic analyses (LC206, 5'-GGCCATGGGCTCATCTTAAG-3', *Escherichia coli* positions 206 to 225) and sequences for *L. ferrooxidans* (LF581, 5'-CGGCCTTTCACCAAAGAC-3', *E. coli* positions 581 to 598) from the Ribosomal Database Project (RDP) and GenBank. The probe for *T. ferrooxidans* was based on RDP and GenBank sequences (TF539; 5'-CAGACCTAACGTACCGCC-3', *E. coli* positions 539 to 556). Domain level probes were Bac 338 (5'-GCTGCCTCCCGTAGGAGT-3', *E. coli* positions 338 to 355), Arch 915 (5'-GTGCTCCCCCGCCAATTCCT-3', *E. coli* positions 915 to 934), and Euk 502 (5'-ACCAGACTTGCCCTCC-3', *E. coli* positions 502 to 517; Alm et al. 1996). Probe design, probe labeling, and hybridization procedures can be found elsewhere (Schrenk et al. 1998; Edwards et al., in press).

Two sites were chosen for comparison here. “B-drift” is located within the sulfide ore-body at the Richmond mine. The “tunnel” site is located at the entrance to the mine, outside of the ore-body. The environmental conditions at these two sites over the course of 1 year (1997) are plotted in Figure 13. At both sites, temperatures are the hottest in January, decreasing through the remainder of the year. This is related to regional precipitation, which is highest in the winter. The high rainfall increases oxygenation of the waters interacting with the sulfides, resulting in increased oxidation rates and hence warmer temperatures because of the exothermic nature of the reaction (Nordstrom and Munoz 1985). Figure 13 shows that the pH at B-drift fluctuates only moderately, with no apparent trend. Among the rest of the Richmond 5-way “drifts,” an increase in average pH rose over the year (0.5–0.9; data not shown). The pH conditions in the “tunnel” reflect this trend, but at a higher pH range (1.4–2.2), which is characteristic of this locality. Conductivity generally increases during the dry summer months at both localities, reflecting increasing ionic strength of the solutions as rainfall decreases. As reflected in Figure 13, environmental conditions at Iron Mountain show considerable seasonal and spatial variation. This allows us to study fluctuations in microbial population as a function of geochemical conditions, as well as investigate the roles of the two best-studied microorganisms associated with AMD, *T. ferrooxidans* and *L. ferrooxidans*, over the range of these conditions.

Selected probing results for two end-member times of year (in terms of geochemical conditions) for the above sites are summarized in Figure 14. The B-drift probing data shown here are for sediment samples and include counts for microorganisms attached to and closely associated with pyritic sediments. The data shown are representative of several trends in microbial populations at this site, which are supported by a larger data set (not shown here). One important observation is that although *T. ferrooxidans* and *L. ferrooxidans* predominate locally at certain sites and geochemical conditions, overall they represent a small proportion of the total microbial population. *T. ferrooxidans* is virtually absent from the sites that are in contact with the sulfide ore-body. Distribution of this species at the Iron Mountain sites is relatively restricted to locations with lower temperatures and more moderate pH conditions, such as found in the tunnel and the runoff streams located peripherally to the

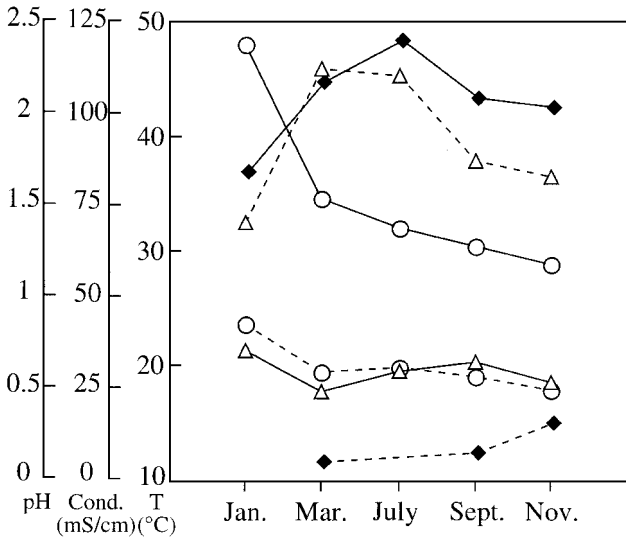


**FIGURE 13** Environmental conditions during 1997 sampling trips to Iron Mountain, CA. Symbols are as follows: circles, temperature; diamonds, conductivity; triangles, pH. Dashed lines represent conditions at the entrance tunnel to the Richmond 5-way mine; solid lines represent conditions at a site inside the Richmond mine (B-drift).

primary acid-generating sites in contact with sulfides (also see Schrenk et al. 1998). Because *T. ferrooxidans* appears primarily to be utilizing solubilized ferrous iron for energy rather than directly attacking sulfide minerals, one might therefore consider it as playing more an opportunistic than a primary role in the generation of AMD. In fact, it may play a beneficial role, as far as environmental damage is concerned, by oxidizing dissolved ferrous iron. This, in turn, induces precipitation of ferric iron oxides, which strongly sorb other metals (such as As). *L. ferrooxidans* is present in higher abundance at sites in contact with the sulfide ore-body, but its distribution is spatially heterogeneous. At some sites within the mine, this species makes up as much as ~70% of the microbial population (slimes; Schrenk et al. 1998); at others, it is virtually absent (sediments; Figure 14, B sed, July). Though its spatial distribution at the site is fairly well predictable, no direct correlation with geochemical conditions within the mine and the presence of *L. ferrooxidans* can yet be made.

A second trend these data reveal is the seasonal occurrence of Archaea. Archaea, which are virtually absent during the high-flow/high-temperature winter months, are quite prevalent in the dry summer months, when metal loads are quite high (Figure 13), and even dominate some localities as shown in B-drift sediments (Figure 14). Eukarya also occur in greater abundance in the summer months, in fact increasing proportionally throughout the year as temperature steadily drops (data not shown). Whether this is temperature- or flow-related is not clear. Eukarya occur primarily as filaments in massive slime streamers, though some protozoa have been observed. The lack of eukarya filaments in the winter months is likely to be in part due to physical removal during the periodic floods that occur after heavy rainfalls and may not be strictly related to geochemical conditions.

## Discussion and Conclusions

The oxidative dissolution of sulfide minerals, and the impact microorganisms can have on this process in nature, have been well studied by aqueous geochemists and microbial ecologists. However, previous studies have generally used a small, possibly nonrepresentative,

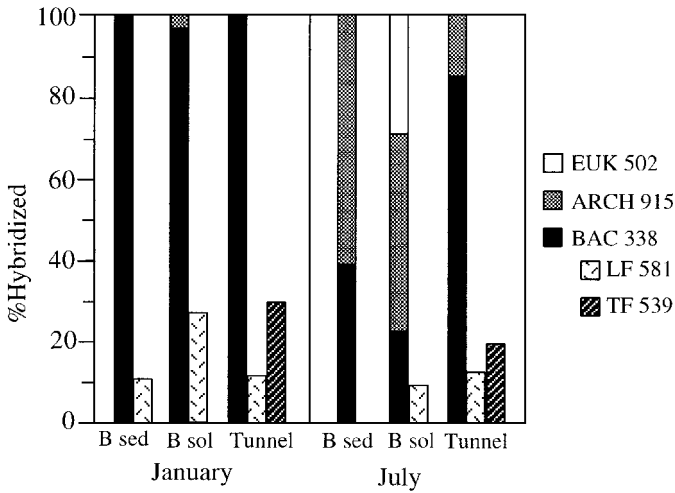


**FIGURE 14** Hybridization results from two sampling trips to Iron Mountain, CA. B refers to B-drift, one of the main flows at the Richmond 5-way mine, located within the sulfide ore-body; Tunnel refers to the entrance tunnel into the Richmond mine, located outside of the ore-body; sed refers to sediment, sol to solution. See Figure 11 for environmental conditions at these sites. Percentages shown have been normalized to the total number of cells that hybridized with the domain probes, thus excluding dead, inactive, or impermeable cells. The first column for each site indicates the proportion of microorganisms in each of the three domains (Bacteria, Archaea, and Eukarya in ascending order). LF, *L. ferrooxidans*; TF, *T. ferrooxidans*.

set of microbes for laboratory studies. Assumptions and simplifications such as these may affect conclusions and ultimately the models developed to predict this acid generation by microorganisms in the environment. Thus, when assessing this process, the first key question to address is, what are the species relevant at acid-generating sites? Numerous methods are now available to answer this, from traditional culturing techniques, to direct phylogenetic analysis of environmental samples without culturing, to FISH. Workers must recognize, however, that biases are introduced by *each* of these methods and that use of all available techniques will provide the most integrated picture of a microbial community.

At Iron Mountain, our 16S analyses have suggested the presence of a mixture of likely species, of poorly understood species, and of species whose presence in the environment is not completely verified. FISH analyses have placed the sequence analysis in context, allowing us to quantitatively demonstrate that *T. ferrooxidans* is not the most important lithotroph in key acid-generating sites and that *L. ferrooxidans* is important but is spatially restricted. Furthermore, probing indicates some significant changes in the balance of species as a function of geochemical conditions, which vary with microenvironment and season. Data also indicate potentially important ecological roles for heterotrophs, including Eukarya, and seasonal significance.

While community analysis provides important information on microbial population distributions, laboratory experiments provide necessary information on how microbial pyrite oxidation takes place, particularly when coupled with in situ field experiments. Our laboratory experiments and parallel field-based surface colonization studies indicate that subsets of chemolithotropic species from the field site can be cultured, which can catalyze pyrite dissolution. Attached species have significant effects on surface chemistry, causing pronounced local pitting that is absent in the presence of exclusively planktonic species. The changes in surface structure and composition that occur during dissolution are controls on

the rate of AMD generation. Our results show that surface deposits form even at these very low pH values because of the high ferric concentrations. Ferric ion also plays an important role in controlling the evolution of surface topography and subsequent dissolution rates.

This study has brought together results from biological, mineralogical, and chemical approaches. It has provided abundant quantitative information, such as the rate of pyrite dissolution at the site of acid generation (at the temperature and pH conditions measured at the site of pyrite weathering and determined with microbes shown to be important in the relevant geochemical environments). We have also quantified surface colonization kinetics and provided information about cell numbers per unit surface area. Initial observations about the ecology of low-pH environments have also been made. Much remains to be learned, particularly with respect to ecology—for example, the interrelation of lithotrophic and heterotrophic organisms, and the relative importance of Archaea. The identity of many species remain unknown. The information to date places the experimental work done in previous studies in context and provides important parameters for predictive models relevant at Iron Mountain and other comparable low-pH AMD sites. Future work on the ecological and chemical aspects is required before geomicrobial remediation strategies can be effectively formulated.

## References

- Altschul SF, Madden TL, Schaeffer AA, Zhang J, Zhang Z, Miller W, Lipman DJ. 1997. Gapped BLAST and PSI-BLAST: a new generation of protein database search programs. *Nucleic Acids Res* 25:3389–3402.
- Amann RI, Ludwig W, Schleifer K. 1995. Phylogenetic identification and in situ detection of individual microbial cells without cultivation. *Microbiol Rev* 59:143–169.
- Barns SM, Fundyga RE, Jeffries MW, Pace NR. 1994. Remarkable archaeal diversity detected in a Yellowstone National Park hot spring environment. *Proc Nat Acad Sci USA* 91:1609–1613.
- Bennet JC, Tributsch H. 1978. Bacterial leaching patterns on pyrite crystal surface. *J Bacteriol* 134:310–326.
- Borneman J, Skroch PW, O'Sullivan KM, Palus JA, Rumjanek NG, Jansen JL, Nienhuis J, Triplett EW. 1996. Molecular microbial diversity of an agricultural soil in Wisconsin. *Appl Environ Microbiol* 62:1935–1943.
- Borneman J, Triplett EW. 1997. Molecular microbial diversity in soils from eastern Amazonia: evidence for unusual microorganisms and microbial population shifts associated with deforestation. *Appl Environ Microbiol* 63:2647–2653.
- Brown AD, Jurinak JJ. 1989. Mechanisms of pyrite oxidation in aqueous mixtures. *J Environ Qual* 18:545–550.
- Clark DA, Norris PR. 1996. *Acidimicrobium ferrooxidans* gen. nov. sp. nov.: mixed-culture ferrous iron oxidation with *Sulfobacillus* species. *Microbiol* 142:172–179.
- Corstjens PL, de Vrind JP, Westbroek P, de Vrind-de Jong EW. 1992. Enzymatic iron oxidation by *Leptothrix discophora*: identification of an iron-oxidizing protein. *Appl Environ Microbiol* 58:450–454.
- Edwards KJ, Gihring TM, Banfield JF. In press. Variations in microbial populations and environmental conditions at an extreme acid mine drainage environment. *Appl Environ Microbiol*.
- Edwards KJ, Schrenk MO, Hamers RJ, Banfield JF. 1998. Microbial oxidation of pyrite: experiments using microorganisms from an extreme acidic environment. *Am Miner* 83:1444–1453.
- Eggleston CM, Ehrhardt JJ, Stumm W. 1996. Surface structural controls on pyrite oxidation kinetics; an XPS-UPS, STM, and modeling study. *Am Miner* 81:1036–1056.
- Emerson D, Moyer C. 1997. Isolation and characterization of novel iron-oxidizing bacteria that grow at circumneutral pH. *Appl Environ Microbiol* 63:4784–4792.
- Evangelou VP, Zhang YL. 1995. A review: pyrite oxidation mechanisms and acid mine drainage prevention. *Crit Rev Environ Sci Technol* 25:141–199.
- Farrelly V, Rainey FA, Stackebrandt E. 1995. Effect of genome size and *rRNA* gene copy number on PCR

- amplification of 16S rRNA genes from a mixture of bacterial species. *Appl Environ Microbiol* 61:2798–2801.
- Garrels RM, Thompson ME. 1960. Oxidation of pyrite by iron sulfate solutions. *Am J Sci* 259:57–67.
- Giovannoni SJ, Britschgi TB, Moyer CL, Field KG. 1990. Genetic diversity in Sargasso Sea bacterioplankton. *Nature* 345:60–63.
- Goebel BM, Stackebrandt E. 1994a. The biotechnological importance of molecular biodiversity studies for metal bioleaching. In: FG Priest, A Ramos-Cormenzana, BJ Tindall, editors. *Bacterial diversity and systematics (FEMS Symp No. 75)*. New York: Plenum Press, p 259–273.
- Goebel BM, Stackebrandt E. 1994b. Cultural and phylogenetic analysis of mixed microbial populations found in natural and commercial bioleaching environments. *Appl Environ Microbiol* 60:1614–1621.
- Goebel BM, Stackebrandt E. 1995. Molecular analysis of the microbial biodiversity in a natural acidic environment. In: CA Jerez, T Vargas, H Toledo, JV Wiertz, editors. *Proc Int Biohydrometallurgy Symp IBS-95, Vol. 2*. Santiago: University of Chile, p 43–52.
- Goldhaber MB. 1983. Experimental study of metastable sulfur oxyanion formation during pyrite oxidation at pH 6–9 and 30°C. *Am J Sci* 283:193–217.
- Helle U, Onken U. 1988. Continuous microbial leaching of a pyritic concentrate by *Leptospirillum*-like bacteria. *Appl Microbiol Biotechnol* 28:553–558.
- Higgins SR, Hamers RJ. 1995. Spatially-resolved electrochemistry of the lead sulfide (galena) surface by electrochemical scanning tunneling microscopy. *Surface Sci* 324:263–281.
- Higgins SR, Hamers RJ. 1996. Chemical dissolution of the galena (001) surface observed using scanning tunneling microscopy. *Geochim Cosmochim Acta* 60:3067–3073.
- Hiraishi A, Kishimoto N, Kosako Y, Wako N, Tano T. 1995. Phylogenetic position of the menaquinone-containing acidophilic chem-organotroph *Acidobacterium capsulatum*. *FEMS Microbiol Lett* 132:91–94.
- Hugenholtz P, Goebel BM, Pace NR. 1998. Impact of culture-independent studies on the emerging view of bacterial diversity. *Appl Environ Microbiol* 180:4765–4774.
- Johnson DB, Roberto FF. 1997. Heterotrophic acidophiles and their roles in the bioleaching of sulfide minerals. In: DE Rawlings, editor. *Biomining: theory, microbes and industrial processes*. Berlin: Springer-Verlag, p 259–279.
- Kapuscinski J. 1995. DAPI: a DNA-specific fluorescent probe. *Biotech Histochem* 70:220–233.
- Kishimoto N, Kosako Y, Tano T. 1991. *Acidobacterium capsulatum*, new genus, new species: an acidophilic chemoorganotrophic bacterium containing menaquinone from acidic mineral environment. *Curr Microbiol* 22:1–8.
- Konishi Y, Asai S, Sakai HK. 1990. Bacterial dissolution of pyrite by *Thiobacillus ferrooxidans*. *Bioprocess Eng* 5:5–17.
- Kuske CR, Barns SM, Busch JD. 1997. Diverse uncultivated bacterial groups from soils of the arid southwestern United States that are present in many geographic regions. *Appl Environ Microbiol* 63:3614–3621.
- Lane DJ, Harrison AP Jr, Stahl DA, Pace B, Giovannoni SJ, Olsen GJ, Pace NR. 1992. Evolutionary relationships among sulfur- and iron-oxidizing eubacteria. *J Bacteriol* 174:269–278.
- Lowson RT. 1982. Aqueous oxidation of pyrite by molecular oxygen. *Chem Rev* 82:461–497.
- Ludwig W, Bauer SH, Bauer M, Held I, Kirchhof G, Schulze R, Huber I, Spring S, Hartmann A, Schleifer KH. 1997. Detection and in situ identification of representatives of a widely distributed new bacterial phylum. *FEMS Microbiol Lett* 153:181–190.
- Maidak BL, Olsen GJ, Larsen N, Overbeek R, McCaughey MJ, Woese CR. 1997. The RDP (Ribosomal Database Project). *Nucleic Acids Res* 25:109–110.
- Markosyan GE. 1972. A new acidophilic iron bacterium *Leptospirillum ferrooxidans*. *Bio Zh Armenii* 25:26.
- Martello DV, Vecchio KS, Diehl JR, Graham RA, Tamilia JP, Pollack SS. 1994. Do dislocations and stacking faults increase the oxidation rate of pyrites? *Geochim Cosmochim Acta* 58:4657–4665.
- McKibben MA, Barnes HL. 1986. Oxidation of pyrite in low temperature acidic solutions: rate laws and surface textures. *Geochim Cosmochim Acta* 50:1509–1520.
- Mernagh TP, Trudu AG. 1993. A laser Raman microprobe of some geologically important sulphide minerals. *Chem Geol* 103:113–127.

- Moses CO, Nordstrom DK, Herman JS, Mills AL. 1987. Aqueous pyrite oxidation by dissolved oxygen and ferric iron. *Geochim Cosmochim Acta* 51:1561–1572.
- Mycroft JR, Bancroft GM, McIntyre NS, Lorimer JW, Hill IR. 1990. Detection of sulphur and polysulphides on electrochemically oxidized pyrite surfaces by x-ray photoelectron spectroscopy and Raman spectroscopy. *J Electroanal Chem* 292:139–152.
- Nesbitt HW, Musir IJ. 1994. X-ray photoelectron spectroscopic study of a pristine pyrite surface reacted with water vapor. *Geochim Cosmochim Acta* 58:4667–4679.
- Nordstrom DK. 1982. Aqueous pyrite oxidation and the consequent formation of secondary iron minerals. In: JA Kittrick, DS Fanning, LR Hossner, DM Kral, H Sherri, editors. *Acid sulfate weathering; proceedings of a symposium*. SSSA Special Publication 10. Madison, WI: Soil Science Society of America, p 37–56.
- Nordstrom DK, Alpers N. In press. Geochemistry of acid mine waters. In: G Plumlee, M Logsdon, editors. *Reviews in Economic Geology*, Vol. 6. Society of Economic Geologist.
- Nordstrom DK, Munoz JL. 1985. *Geochemical thermodynamics*. Menlo Park, CA: Benjamin/Cummings.
- Nordstrom DK, Southam G. 1997. Geomicrobiology of sulfide mineral oxidation. In: JF Banfield, KH Nealson, editors. *Geomicrobiology: interactions between microbes and minerals (Reviews in Mineralogy, Vol. 35)*. Washington, DC: Mineralogical Society of America, p 361–382.
- Norris PR. 1983. Iron and mineral oxidation with *Leptospirillum*-like bacteria. In: F Rossi, AE Torma, editors. *Recent progress in biohydrometallurgy*. Iglesias: Associazione Mineraria Sarda, p 83–96.
- Norris PR. 1988. Bacterial diversity in reactor mineral leaching. In: G Durand, L Bobichon, J Florent, editors. *Proc 8th Int Biotechnology Symp*. Paris: Société Française de Microbiologie, p 1119–1130.
- Pace RN, Stahl DA, Lane DJ, Olsen GJ. 1986. The analysis of natural microbial population by ribosomal RNA sequences. *Adv Microbial Ecol* 9:1–55.
- Pizarro J, Jedlicki E, Orellana O, Romero J, Espejo RT. 1996. Bacterial populations in samples of bioleached copper ore as revealed by analysis of DNA obtained before and after cultivation. *Appl Environ Microbiol* 62:1223–1328.
- Rawlings DE. 1995. Restriction enzyme analysis of 16S rRNA genes for the rapid identification of *Thiobacillus ferrooxidans*, *Thiobacillus thiooxidans* and *Leptospirillum ferrooxidans* strains in leaching environments. In: CA Jerez, T Vargas, H Toledo, JV Wiertz, editors. *Proc Int Biohydrometallurgy Symp IBS-95, Vol. 2*. Santiago: University of Chile, p 9–17.
- Rawlings DE, Kusano T. 1994. Molecular genetics of *Thiobacillus ferrooxidans*. *Microbiol Rev* 59:39–55.
- Reysenbach AL, Giver LJ, Wickham GS, Pace NR. 1992. Differential amplification of rRNA genes by polymerase chain reaction. *Appl Environ Microbiol* 58:3417–3418.
- Rheims H, Sproun C, Rainey FA, Stackenbrandt E. 1996. Molecular biological evidence for the occurrence of uncultured members of the actinomycete line of descent in different environments and geographical locations. *Microbiology* 142:2863–2870.
- Rimstidt DJ, Newcomb WD. 1992. Measurement and analysis of rate data: the rate of reaction of ferric iron with pyrite. *Geochim Cosmochim Acta* 57:1919–1934.
- Rodgers TM. 1996. Bacterial diversity in acid mine drainage from Iron Mountain, Shasta County, California: a 16S ribosomal RNA approach. MS Thesis, Department of Geology & Geophysics, University of Wisconsin-Madison.
- Rodgers TM, Banfield JF, Alpers CN, Goodman RM. 1996. Bacterial diversity in acid mine drainage from Iron Mountain, Shasta Co., California; a ribosomal DNA approach. Abstracts with Programs, Geological Society of America 28:35.
- Runnells DD, Shepard TA, Angino EE. 1993. Metals in water—determining natural background concentrations in mineralized areas. *Environ Sci Technol* 26:2316–2322.
- Sand W, Gerke T, Hallmann R, Schippers A. 1995. Sulfur chemistry, biofilm, and the (in)direct attack mechanism—a critical evaluation of bacterial leaching. *Appl Microbiol Biotechnol* 43:961–966.
- Sand W, Gerke T, Jozso P, Shippers A. 1997. Novel mechanism for bioleaching of metal sulfides. In: *Proc Int Biohydrometallurgy Symp IBS97, Biomin97*. South Australia: Australian Mineral Foundation, p QP2.1–QP2.10.

- Sand W, Rohde K, Sobotke B, Zenneck C. 1992. Evaluation of *Leptospirillum ferrooxidans* for leaching. *Appl Environ Microbiol* 58:85–92.
- Sasaki K. 1994. Effect of grinding on the rate of oxidation of pyrite by oxygen in acid solutions. *Geochim Cosmochim Acta* 58:4649–4655.
- Sasaki K, Masami T, Ohtsuka T, Konno H. 1995. Confirmation of a sulfur-rich layer on pyrite after oxidative dissolution by Fe(III) ions around pH 2. *Geochim Cosmochim Acta* 59:3155–3158.
- Schippers A, Jozsa PG, Sand W. 1996. Sulfur chemistry in bacterial leaching of pyrite. *Appl Environ Microbiol* 62:3424–3431.
- Schrenk MO, Edwards KJ, Goodman RM, Hamers RJ, Banfield JF. 1998. Distribution of *Thiobacillus ferrooxidans* and *Leptospirillum ferrooxidans*: implications for generations of acid mine drainage. *Science* 279:1519–1522.
- Silverman MP, Ehrlich HK. 1964. Microbial formation and degradation of minerals. *Adv Appl Microbiol* 6:153–206.
- Singer PC, Stumm W. 1968. Kinetics of the oxidation of ferrous iron. 2nd Symp Coal Mine Drainage Research. Pittsburgh: National Coal Association/Bituminous Coal Research, p 12–34.
- Stackebrandt E, Goebel BM. 1994. Taxonomic note: a place for DNA–DNA reassociation and 16S rRNA sequence analysis in the present species definition in bacteriology. *Int J Syst Bacteriol* 44:846–849.
- Stackebrandt E, Liesack W, Goebel BM. 1993. Bacterial diversity in a soil sample from a subtropical Australian environment as determined by 16S rDNA analysis. *FASEB J* 7:232–236.
- Stackebrandt E, Rainey FA, Ward-Rainey NL. 1997. Proposal for a new hierarchic classification system, *Actinobacteria classis* nov. *Int J Syst Bacteriol* 47:479–491.
- Stokes HN. 1901. On pyrite and marcasite. US Geol Survey Bull 186.
- Strunk O, Ludwig W. 1995. ARB—a software environment for sequence data. Department of Microbiology, Technical University of Munich, Germany.
- Straub KL, Benz M, Schink B, Widdel F. 1996. Anaerobic, nitrate-dependent microbial oxidation of ferrous iron. *Appl Environ Microbiol* 62:1458–1460.
- Suzuki MT, Giovannoni SJ. 1996. Bias caused by template annealing in the amplification of mixtures of 16S rRNA genes by PCR. *Appl Environ Microbiol* 62:625–630.
- Tanner MA, Goebel BM, Dojka MA, Pace NR. 1998. Specific ribosomal DNA sequences from diverse environmental settings correlate with experimental contaminants. *Appl Environ Microbiol* 64:3110–3113.
- Taylor BE, Wheeler MC, Nordstrom DK. 1984a. Stable isotope geochemistry of acid mine drainage: experimental oxidation of pyrite. *Geochim Cosmochim Acta* 48:2669–2678.
- Taylor BE, Wheeler MC, Nordstrom DK. 1984b. Isotope composition of sulfate in acid mine drainage as measure of bacterial oxidation. *Nature* 308:333–344.
- Tebo BM, Ghiorse WC, van Waasbergen LG, Seiring PL, Caspi R. 1997. Bacterially-mediated mineral formation: Insights into manganese (II) oxidation from molecular genetic and biochemical studies. In: JF Banfield, KH Nealson, editors. *Geomicrobiology: interactions between microbes and minerals* (Reviews in Mineralogy, Vol. 35). Washington, DC: Mineralogical Society of America, p 225–260.
- Thibeau RJ, Brown CW, Heidersbach RH. 1978. Raman spectra of possible corrosion products of iron. *Appl Spectrosc* 32:532–535.
- Vásquez M, Espejo RT. 1997. Chemolithotrophic bacteria in copper ores leached at high sulfuric acid concentrations. *Appl Environ Microbiol* 63:332–334.
- Wang Y, Zhang Z, Ramanan N. 1997. The actinomycete *Thermobispora bispora* contains two distinct types of transcriptionally active 16S rRNA genes. *J Bacteriol* 179:3270–3276.
- Wiersma CL, Rimstidt JD. 1984. Rates of reactions and marcasite with ferric iron at pH 2. *Geochim Cosmochim Acta* 48:85–92.
- Williamson MA, Rimstidt JD. 1994. The kinetics and electrochemical rate-determining step of aqueous pyrite oxidation. *Geochim Cosmochim Acta* 58:5443–5454.
- Wilson IG. 1997. Inhibition and facilitation of nucleic acid amplification. *Appl Environ Microbiol* 63:3741–3751.
- Wise MG, McAuthur JV, Shimkets LJ. 1997. Bacterial diversity of a Carolina bay as determined by 16S rRNA gene analysis: confirmation of novel taxa. *Appl Environ Microbiol* 63:1505–1514.